International Journal of Engineering Inventions
e-ISSN: 2278-7461, p-ISSN: 2319-6491
Volume 11, Issue 8 [August. 2022] PP: 65-74

Performance Evaluation of Different Configuration of Sensible Storage.

I.SYED SADIQ NAWAZ [1], V.NARESH [2], S.PAZHANI[3]
[1 –] *PG STUDENT, BHARATHIDASAN ENGINEERING COLLEGE, NATTRAMPALLI.*
[2-] *ASSISTANT PROFESSOR, BHARATHIDASAN ENGINEERING COLLEGE, NATTRAMPALLI.*
[3-] *ASSISTANT PROFESSOR, BHARATHIDASAN ENGINEERING COLLEGE, NATTRAMPALLI.*

ABSTRACT

Evacuated tube (ET) solar collectors are utilized in all climatic condition for harnessing solar energy. This work aims to investigate thermal performance of ET with compound parabolic concentrator, integrated with multiple phase change material based thermal energy storage (TES) system. The PCMs have been selected based on degree of stratification in sensible heat storage configuration under constant heat load conditions. Charging experiments have been performed under three different TES configurations viz. sensible heat storage, three ('Case 1') and five ('Case 2') PCMs, using water as the heat transfer fluid (HTF). AHigher temperature driving potential is attained during melting of PCM, augmenting the energy storage by 41% than the sensible heat storage.Higher stratification number in 'Case 2' reveals the significant of multiple PCMs in improving the charging efficiency of TES system. Cascaded arrangement of PCMs facilitates the augmenting the energy charging supply the HTF at lower temperature in comparison with sensible heat storage. Theinstantaneous thermal efficiency of collector with Case 2 configuration has been as high as 58 %, storing 27 MJ/day.Use of ET CPC and TES system with cascaded arrangement of PCMs finds potential application in water heating system.

KEYWORDS: evacuated tube collector, CPC collector, multiple phase change materials, thermal efficiency, stratification number, solar water heating

---

Date of Submission: 07-08-2022 Date of Acceptance: 22-08-2022

---

1. INTRODUCTION

Effective utilization of abundantly available solar energy with intermittent nature depends on the selection of appropriate energy storage methods to reduce the mismatch between energy demand and supply. Thermal energy storage (TES) system is the most promising one, as the stored energy can be directly consumed in the form of hot or cold energy, minimizing the energy losses during conversion in different applications.[1,2] Energy can be stored either in the form of sensible or latent heat; the later possesses a higher energy storage density, capable of storing or retrieving energy in a nearby isothermal condition.[3-4]**.** The phase change materials (PCM) are ubiquitously utilized in latent heat thermal energy storage systems and numerous PCMs are available under the categories of organic, inorganic and eutectic mixtures. Among them, paraffins exhibit the desired phase change characteristics of congruent melting and solidification with a minimal degree of sub-cooling. However, their inherent low thermal transport properties, particularly thermal conductivity inhibit the heat transfer during the phase change. Different passive methods such as providing fins, addition of high conductive solid particles at micro or nanoscale and impregnation of porous media substantially enhance the thermal conductivity of PCMs[5-].[6]Nevertheless, the major drawbacks like increase in weight and settlement of solid particles over periodic thermal cycling are encountered in the system-level applications.

The use of CPC in the solar collector improves the amount of solar energy collection and the cascaded arrangement of PCMs in TES systemfacilitates the high degree of stratification for effective charging in water heating application.To the best of authors' knowledge, no experimental study has been reported on augmentation of thermal performance of solar water heating system with incorporation ofCPCand multiplePCM based TES system.In view of the above, the present work aims to investigate the thermal performance of ET-CPC solar collector paired with different configurations of the TES system under real-time experimental conditions.Initially, the stratification studies have been carried outin the sensible TES system under constant

heat load conditions for selecting the appropriate PCMs, followed bythe charging experiments in different TES configurationswith the proposed ET-CPC solar collector.

2. SIMULATION DESCRIPTIONS

Figure 1 (a) illustrates the schematic arrangement of the experimental systemthat includes the ET-CPC solar collector, TES system, buffer storage tank and centrifugal pump. The ET-CPC solar collector uses eight evacuated tubes (ET), made of borosilicate glassas the absorbers andeach tube is of 0.05 m diameter, 0.002 m thickness and 1.8 m length. TheseETs have a high light transmittance of 0.91 and a U-type copper tube of 8.5 mm diameter is housed inside each glass tube is shown in Figure 1 (b). The copper tubes are interconnected in series forming the serpentine arrangement. The CPCs are made of aluminum sheets with a concentration ratio of 1.2, having a half-acceptance angle of 55° and the cross-sectional structure of the collector module is shown in Figure 1 (c). The CPCs with the trough-like profile are placed 20 mm below the ET tubes to minimize the reflection losses. The overall size of the ET-CPC collector unit is 1.8 × 1.63 × 0.5 m, having an aperture area of 2.75 m^2.

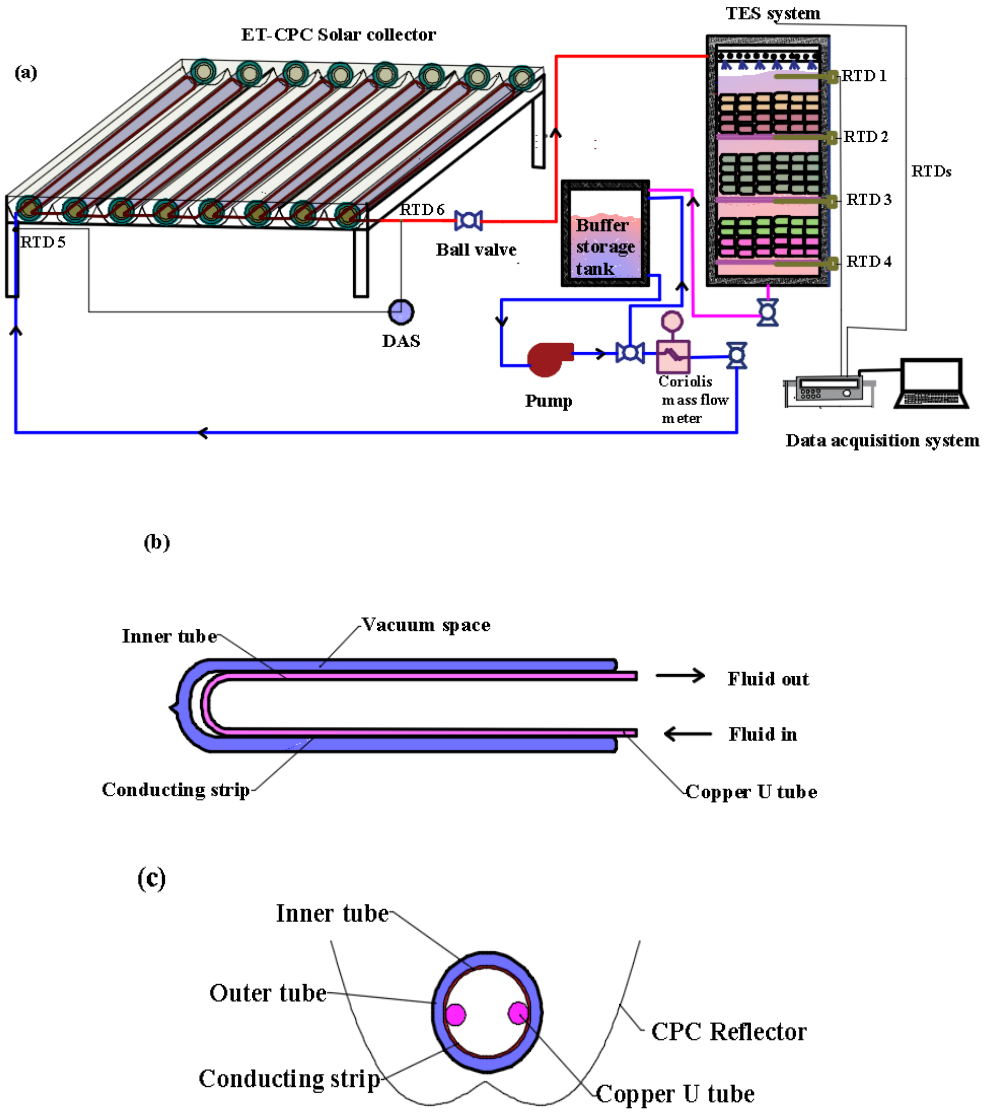

FIGURE 1(a) Schematic layout of the experimental facility; (b) U-type evacuated tube; (c) reflector.

A cylindrical TES system of 0.5 m inner diameter and 1 m height, is fabricated with galvanized iron and ample space is provided at the top of the TES system for placing the sprinklers and resistance temperature detectors (RTD). For the ease of loading and unloading PCMs, the TES system is partitioned into small compartments separated by a perforated plate to support the weight of the encapsulated PCMs, as shown in Figure 2. The outer

surface of the TES system and all connecting pipes are wrapped with the glass wool insulation of 0.06 m thickness for minimizing the heat losses. Water is used as the HTF and circulated in the entire system in a closed loop. The inlet and outlet of ET-CPC collector are connected respectively to the bottom and top of the TES system with thermally insulated pipes. The flow rate of HTF is maintained at 60 kg h^{-1}, monitored continuously by a Coriolis mass flow meter and the excess load on the centrifugal pump during the HTF pumping is minimized through a bypass line. The required PCMs mass is filled in cylindrical capsules made of aluminum, each having a 45 mm inner diameter and 110 mm height. The filling of PCMs is up to 90 % of capsule volume for accommodating the change in volume of the PCM during the melting and the capsules are sealed securely with a cap. Three hundred and sixty such cylindrical capsules are employed and packed in the TES system, maintaining a bed porosity of 56 %. To measure the transient temperature variation of PCMs inside the encapsulation, the RTDs are placed inside two capsules – one at the top and the other at the bottom of each PCM zone. The temperature of the HTF is continuously measured every 1 min at the inlet and outlet of the solar collector and additionally at four different locations (x/L = 0.05,0.35,0.65 and 0.95) in the TES system. For the equal distribution of PCM mass, the TES system is fragmented into three; zone 1- (x/L= 0.05 - 0.35), zone 2- (x/L= 0.35 - 0.65) and zone 3- (x/L= 0.65-0.95). The test facility is located at the roof top of 'Thermal sciences block,' Anna University, Chennai (Latitude 13°00`29'' N and Longitude 80°13`06'' E) and the photographic view of the facility is shown in Figure 3.

Simulation were carried out in May 2019, by orienting the ET – CPC solar collector in the East - West direction. At the start of the charging experiment, the hot HTF coming out from the solar collector was uniformly distributed from the top through the sprinklers into the packed bed TES system. During the flow of HTF, it's mixing with the water occupying the void space in each zone causes an increase in temperature at that particular location, simultaneously transferring the heat to the PCMs. The HTF was recirculated to the inlet of the solar collector for the subsequent charging cycles. The charging experiments were carried out with two different configurations (three and five PCMs) as shown in Figure 2 and the duration of all the experiments was from 08.00 h till 17.00 h. The meteorological data like solar radiation, wind velocity and ambient temperature were continuously recorded in the weather station, installed near the test facility.

3. DATA ANALYSIS

Thermal performance parameterslike instantaneous energy stored, stratification number and collector efficiency are evaluatedand analyzed from the experimental data.Useful heat gained by the HTF, flowing through the ET-CPC solar collector is determined using the following Equation (1).

$$Q_u = \dot{m}_f \times c_f \times \Delta T \times dt \qquad (1)$$

where, $\dot{m}_f$ -mass flow rate (kg s^{-1}), c_f -specific heat (kJ kg^{-1} K^{-1}),ΔT-temperature difference of the HTF (K) and dt - time interval (s).

The amount of energy stored in each PCM zone of the TES system is calculated using Equation (1), by substituting the measured ' ΔT 'across each PCM zone and the total energy stored is given below.

$$Q_s = Q_1 + Q_2 + Q_3 \qquad (2)$$

where,Q_1, Q_2 and Q_3 represent the energy stored ineach PCM zone.

The ratio of mean temperature gradient at each time interval to that of the beginning (t = 0) is stratification number, coined by Seara et al[25] andit can be expressed as,

$$Str = \frac{(\partial T / \partial y)_t}{(\partial T / \partial y)_{t=0}} \qquad (3)$$

$$\frac{\partial T}{\partial y} = \frac{1}{J-1}\sum_{j=1}^{j-1}\frac{T_{j+1} - T_j}{\Delta y} \qquad (4)$$

where, 'J' represents the number of locations considered in the TES system and for the present case, J = 4.

Instantaneous collector thermal efficiency (η_{sc}) is defined as the ratio of the useful heat gain to the incident solar radiation on the aperture area and it is given by,

$$\eta_{isc} = \frac{Q_u}{A_a G_t} \qquad (5)$$

where, A_a - aperture area (m^2) and G_t - total incident radiation on aperture area (W m^{-2}).
The useful heat energy gain can also be expressed in terms of 'F_R' and 'U_L', as given by

$$Q_u = F_R\left[SA_a - A_r U_L(T_{mp} - T_{amb})\right] \quad (6)$$

where, 'F_R' – heat removal factor, S - absorbed solar energy (W m^{-2}), A_a - aperture area (m^2), A_r - receiver-absorber area (m^2) and U_L- overall loss coefficient (W m^{-2} K^{-1}). T_{mp}- mean plate temperature (°C)
It is essential to determine the overall efficiency of the system, which is the product of charging efficiency (η_c) and instantaneous collector thermal efficiency (η_{sc}).

$$\eta_o = \eta_c \times \eta_{sc} \quad (7)$$

The charging efficiency (η_c) of the TES system is the ratio of energy stored to the energy available at the input of the TES system.

$$\eta_c = \frac{Q_s}{Q_u} \quad (8)$$

where, 'Q_u'is the useful heat gained by the HTF from the solar collector as given in Equation (1).

4. RESULTS AND DISCUSSION

4.1. Instantaneous energy stored

Experiments have been carried out in the test facility under sensible heat storage, case 1 and case 2 respectively on 5th, 15th and 16th of May 2019.The corresponding measured global radiation and ambient temperatureduring the experiments are given in Figure5. The intensity of solar radiation and ambient temperature range between 303 – 995 W m^{-2} and 32 – 35 °C respectively.

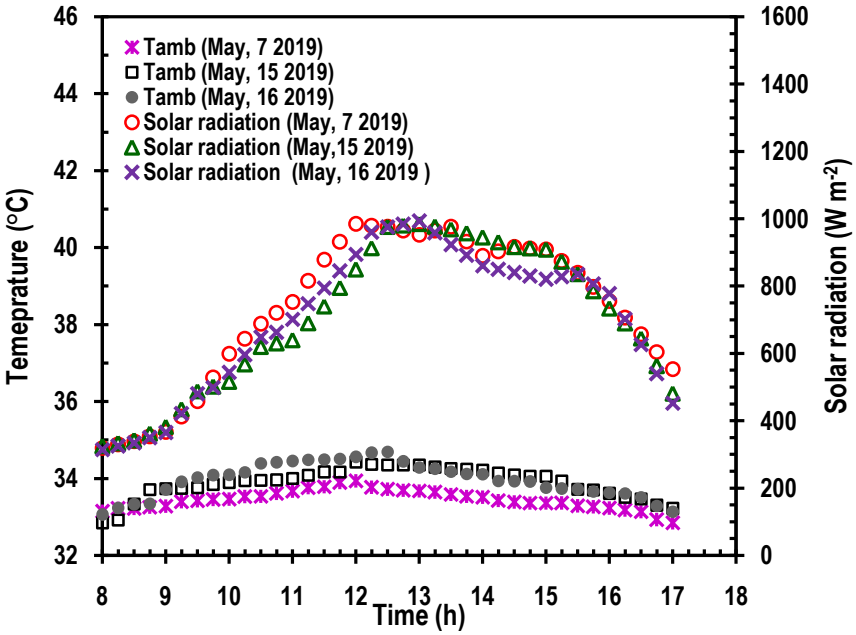

FIGURE 5 Measured solar radiation intensity and ambient temperature

To explore the effects of PCM addition, the instantaneousenergy stored is evaluated for sensible heat storage, 'Case 1' and 'Case 2' configurations using Equation (1) and the results are compared in Figure6. The amount of energy stored at any particular time interval is proportional to the heat output from the collector in all the configurations. For the sensible heat storage configuration, a steady increase in instantaneous energy stored is observed until 12.00 h, mainly from the increase in solar radiation. However, a declining trend is perceivedtill the end of the experiment, cumulatingan energy storage of 15.4 MJ in a day. On taking a closer look at different locations of the TES system, the charging rate is faster in the topmost region (x/L=0.05) and tends to decrease with further charging due to the mixing of the HTF. As shown in Figure 7, a thermal stratification of 2 - 4 °C is exhibited between the adjacent locations in the case of sensible heat storage configuration between 13.00 h – 15.00 h. Later on, this stratification is diminished gradually by the reduced solar radiation and enhanced convective currents, indicating the thermal destratification in the TES system. The instantaneous energy stored tends to decreaseabruptly

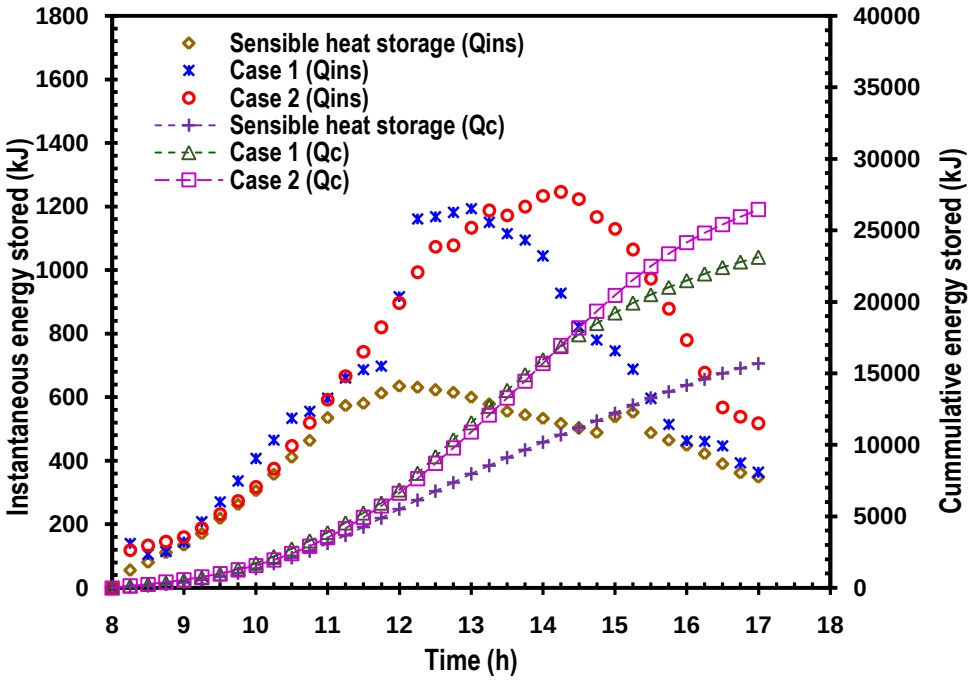

FIGURE 6 Energy stored in different configurations of TES system

and the cumulative energy storage of 4.5 MJ, 5.5 MJ and 5.3 MJ is stored between the locations x/L = 0.05 - 0.35, 0.35 - 0.65 and 0.65 - 0.95, respectively. As can be noticedfor 'Case 1' and 'Case 2', the energy stored nearly equals tothe sensible heat storage configuration between 8.00 h - 11.00 h, heating the PCMssensibly inthe solid region. The cascaded arrangementof PCMs facilitates an enhanced heat transfer during the melting, storing a larger amount of energy by maintaining the required temperature driving potential between the HTF and PCMs. A major portion of PCMs melts during 12.00 h - 16.30 h at all the locations for 'Case 1', sustaining the higher temperature driving potential of 11 °C, 24 °C and 28 °C at x/L = 0.05, 0.35 and 0.65, respectively. The increasing trend of the HTF temperature during this period is much higher for 'Case 1' and 'Case 2' than the sensible heat storage configuration, mainly due to the melting of PCMs in a nearby isothermal manner. Further, the cascading of the PCMs with narrow melting temperatures in 'Case 2' augments the energy stored by 41 % and12 % than the sensible heat storage and 'Case 1' configurations, respectively. On the other hand, the energy stored drops at a faster rate during 14.50 h - 17.00 h, primarily due to two reasons; the sensible heating of PCMs in the liquid region causing a reduction in the temperature driving potential and a greatly reduced available solar radiation. In conclusion, thermal performance of the TES system is improved passively by storing a higher amount of energy through the multiple PCMs arrangement with narrow melting temperatures.

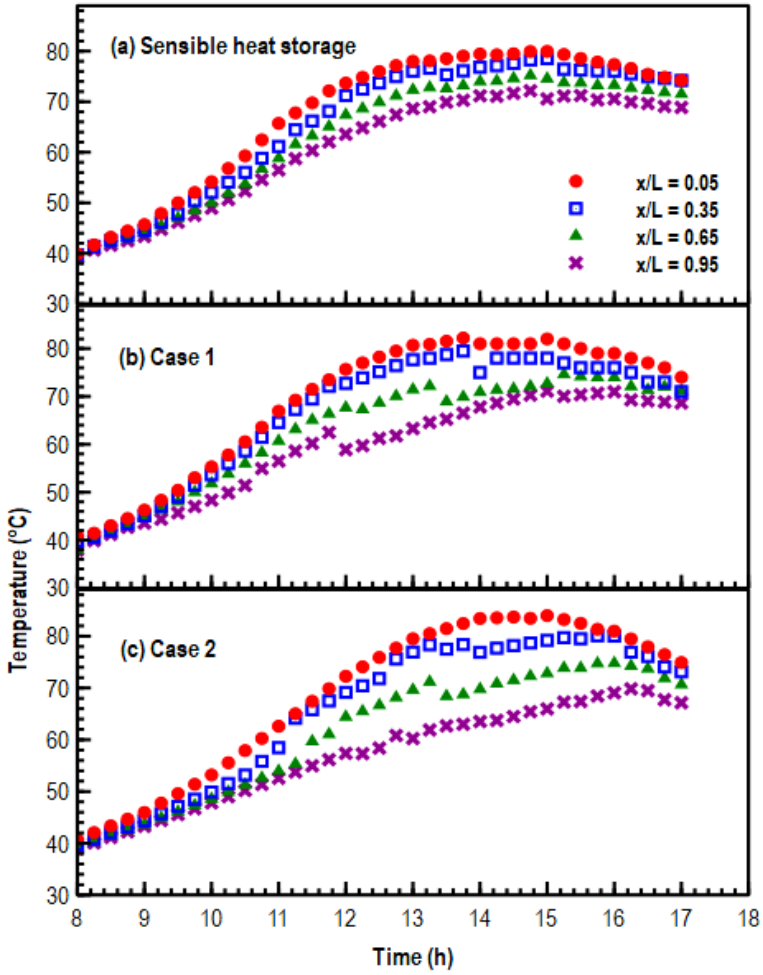

FIGURE 7 T – t history of HTF at different locations in the TES system

4.3 Stratification number

This dimensionless number characterizes the ratio of instantaneous temperature gradient to temperature gradient at the beginning of charging process. Figure 8 presents the variation of stratification number with respect to non-dimensional time, defined as $\tau = t_{ins} / t_{tot}$, for three TES configurations. The profiles exhibit initially an increasing trend, reaching the maximum and a subsequent decline as the charging proceeds for all the configurations. During the initial periods, the existence of a high thermal gradient increases the stratification number, attaining the maximum of 14, 26.8 and 27 for sensible heat storage, 'Case1' and 'Case 2' configurations, respectively. The increase in stratification numberwith the addition of PCMs results from the existence of a high thermal gradient in 'Case1' and 'Case 2'and the corresponding values are found to be 17.7°C $m^{-1}$and 19.8°C m^{-1}on comparing with the baseline case of 10.2 °C $m^{-1}$for the sensible heat storage. This improvement in thermal stratification can be explained by the specific placement of the PCMs with a narrow melting temperature range and also the presence of aluminum capsules.

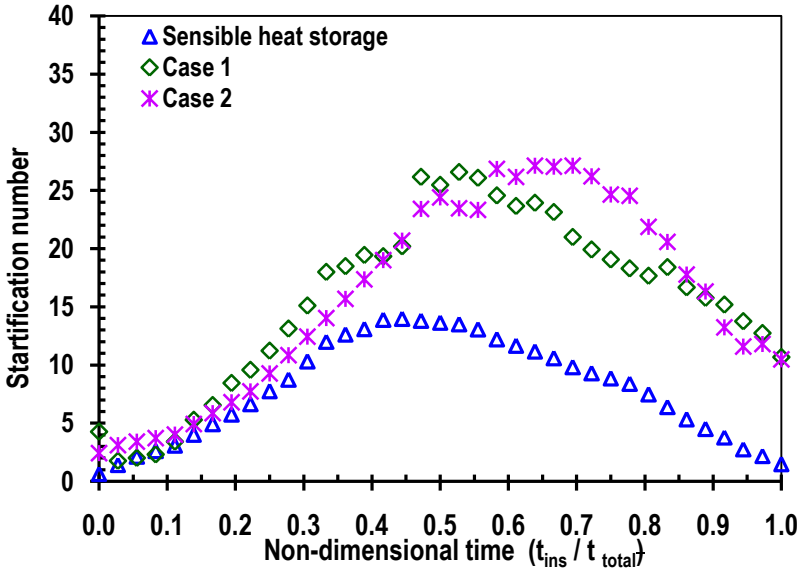

FIGURE 8 Variation of stratification number

A diminishing trend of stratification number is noticed as charging advances,but with the higher values in 'Case1' and 'Case 2' than the sensible heat storage configuration. Thistrend can be attributed to the predominant effects of mixing forces due to the continuous circulation of HTF over a period of time and reduced solar intensity. From the above analysis, it is established that the integration of multiple PCMs improves the charging efficiency of the TES system though the higher thermal stratification.

4.4 Instantaneous thermal efficiency

Figure 9 show the temperature variation of HTF inlet of solar collector for different configuration of TES system. Here, it should be pointed out that the HTF temperature at the collector inlet drops sharply around 12.00 h in 'Case 1', resulting from the melting of PCMs in the TES system. Due to the supply of HTF at the relatively low temperatures to the solar collector as noticed in Figure 8 (b), the convection heat losses from the collector decrease significantly, attaining a peak thermal efficiency of 49 % and 58 % in 'Case 1' and 'Case 2', respectively. The higher collector efficiency for 'Case 2' is solely due to the augmented energy gain in the collector, resulting from the supply of HTF relatively at low temperatures with the cascaded arrangement of PCMs. As time proceeds, the thermal efficiency decreases gradually for all cases, but the solar collector paired with 'Case 2' shows the higher thermal efficiency, in spite of reduced solar radiation, particularly between 15.00 h – 17.00 h. Thermal efficiencies of the ET-CPC solar collector calculated from Equation (5) for three configurations are compared in Figure 10. As can be seen, the ET-CPC solar collector performs better when integrated with the TES system in 'Case 1' and 'Case 2' than sensible heat storage, showing an increasing trend of thermal efficiencies from the start of the experimentation. Similar trend of thermal efficiency enhancement was reported in the case of solar flat plate collector integrated with TES system using single[26] and three PCMs configuration[27].

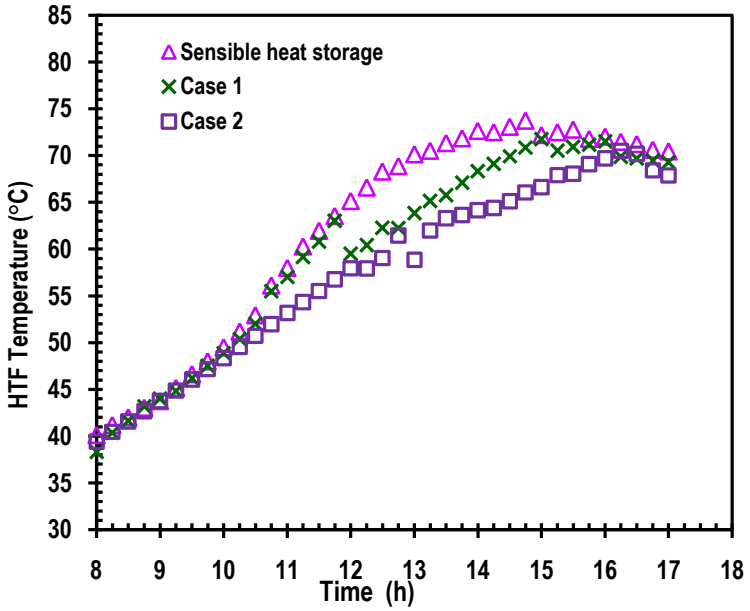

FIGURE 9HTF temperature at collector inlet with local time.

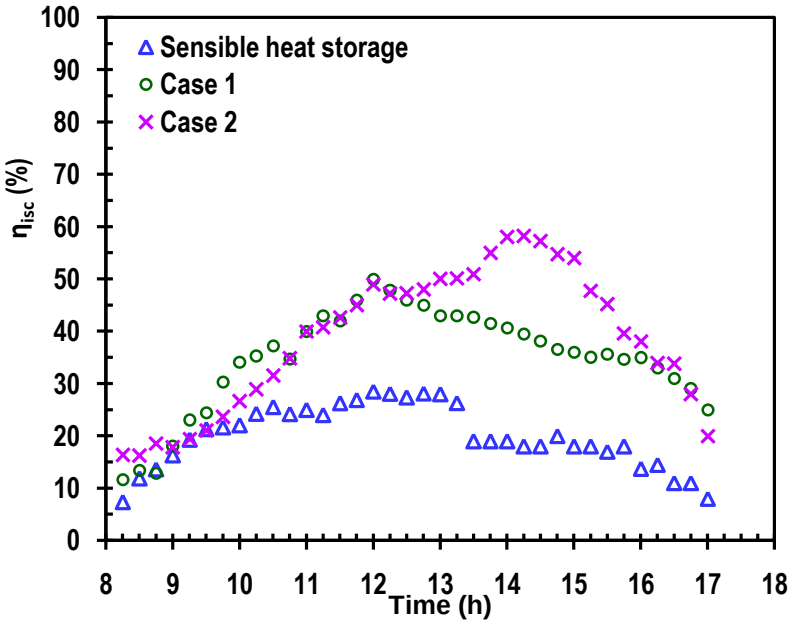

FIGURE 10 Instantaneous thermal efficiency of the collector

For a better overview, the thermal efficiency is plotted with respect to heat loss parameter, defines as $\left[\frac{T_{mean}-T_a}{G_t}\right]$, between11.00 h – 17.00 h, as depicted in Figure 11.The slope of the curve representing 'F_RU_L/C_R' is found to be the lowest in 'Case 2', indicating the minimal overall heat losses compared to other configurations. The heat transfer rate inside the absorber tubes is augmented with lower 'F_RU_L/C_R' thereby increasing the thermal efficiency of the solar collector. As noticed, thermal efficiency drops with an increase in heat loss parameter, emerging from the decrease in thermal resistance between the outer surface and the evacuated tubes. The intercept with the vertical axis denoting '$F_R\eta_o$' of the collector is 0.52, 0.69 and 0.7 paired with sensible heat storage, 'Case 1' and 'Case 2', respectively.

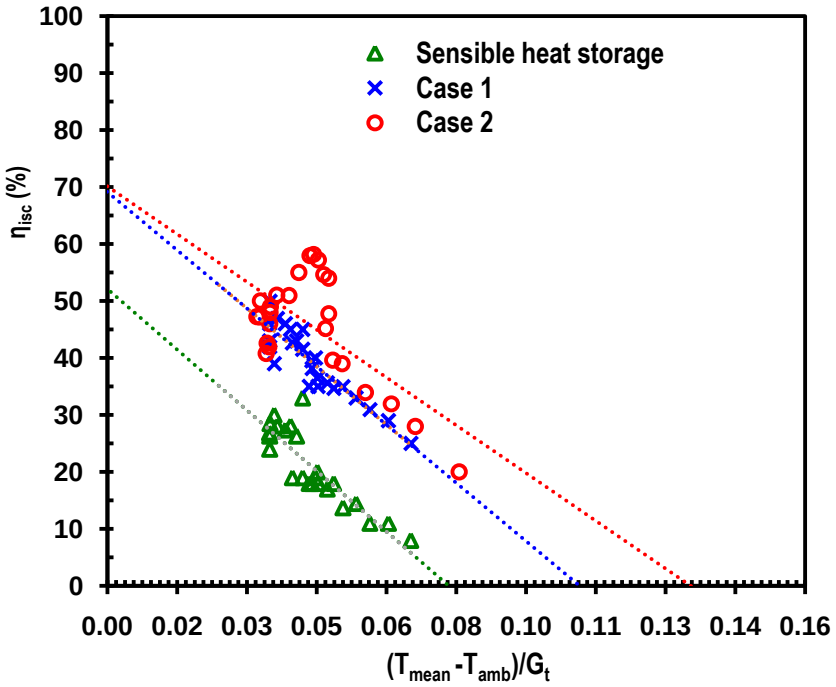

FIGURE 11 Thermal efficiency as the function of loss coefficient

For establishing the advantages of employing CPC and the thermal energy storage system, the present results are compared with the obtained results from a similar configuration of solar collector under Indian climatic conditions.[28] For a given collector area, the thermal efficiency of the solar collector in the present study is higher, demonstrating the predominant role of the multiple PCMs based TES system. Furthermore, the results of Zambolin et al[29] using an evacuated tube collector of aperture area of 3.5 m^2 exhibited the lower thermal efficiency than the present study, signifying the functional enhancement by the CPC. The distinctive advantage of the CPC solar collector is the minimum thermal losses, which are inversely proportional to its concentration ratio and the lower values of 'F_RU_L/C_R' in 'Case 2' ultimately improve the thermal efficiency of the ET-CPC solar collector. Considering the improved thermal efficiency of the ET-CPC collector for 'Case 2', the overall efficiency of the system is enhanced by 8 % and 23 % than 'Case 1' and sensible heat storage configurations, respectively. In light of the above discussion, the synergetic effects of multiple PCMs with a suitable cascaded configuration and compound parabolic concentrator will be beneficial towards the development of a solar-based water heating system with enhanced overall efficiency.

5. CONCLUSION

This study reports the thermal performance of the ET-CPC solar collector through the integration of the TES system configured with three PCMs ('Case 1') and five PCMs ('Case 2'). The melting temperature of the cascaded layered PCMs is selected based on the degree of stratification, arranged in the descending order of the melting points from top to bottom in the TES system. Results of charging experiments revealthat the multiple PCMs configurations introduce a desired temperature driving potential for effective charging, fetching a higher temperature difference of HTF across the TES system. Consequently, an enhancement in energy storage of 41 % and 12 % is accomplished in 'Case 2' compared to sensible heat storage and 'Case1', respectively. Stratification number of 'Case 2' is higher than the other two configurations, establishing a better thermal stratification with the appropriate placement of PCMs. Pairing the ET-CPC solar collector with both multiple PCM configurations progressively increases the thermal efficiency with the circulation of HTFat low temperatures to the collector. Theobtained value of '$F_R\eta_o$' for ET-CPC solar collector with 'Case1' and 'Case 2' is almost the same but the lower value of 'F_RU_L/C_R' in 'Case 2' indicates a reduced heat loss coefficient. It is concluded that the combined effects of the CPC and multiple PCMs based TES system facilitates the development of an efficient solarbased water heating systems for various domestic and industrial applications.

REFERENCES

[1]. Matos CR, Carneiro JF, Silva PP. Overview of large-scale underground energy storage technologies for integration of renewable energies and criteria for reservoir identification. Journal of Energy Storage. 2019; 21:241-58.

[2]. Kumar GS, Nagarajan D, Chidambaram LA, Kumaresan V, Ding Y, Velraj R. Role of PCM addition on stratification behavior in a thermal storage tank–An experimental study. Energy. 2016; 115:1168-78.

[3]. Suresh C, Saini RP. Thermal performance of sensible and latent heat thermal energy storage systems. International Journal of Energy Research. 2020; 44(6):4743-58.

[4]. Ali H M. Recent advancements in PV cooling and efficiency enhancement integrating phase change materials based systems – A comprehensive review. Solar Energy. 2020, 197:163-198

[5]. Tariq SL, Ali H M, Akram MA, Janjua MM, Ahmadlouydarab M . Nanoparticles enhanced phase change materials (NePCMs)-A recent review. Applied Thermal Engineering 2020, 176:115305.

[6]. Karthikeyan S, Solomon GR, Kumaresan V, Velraj R. Parametric studies on packed bed storage unit filled with PCM encapsulated spherical containers for low temperature solar air heating applications. Energy conversion and management. 2014; 78:74-80.

[7]. Farid MM, Kim Y, Kansawa A. Thermal performance of a heat storage module using PCM's with different melting temperature: Experimental. Journal of Solar Energy Engineering, 1990; 112:125–31.

[8]. Watanabe T, Kikuchi H, Kanzawa A. Enhancement of charging and discharging rates in a latent heat storage system by use of PCM with different melting temperatures. Heat Recovery Systems and CHP. 1993; 13(1):57-66.

[9]. Michels H, Pitz-Paal R. Cascaded latent heat storage for parabolic trough solar power plants. Solar Energy. 2007; 81(6):829-37.

[10]. Peiró G, Gasia J, Miró L, Cabeza LF. Experimental evaluation at pilot plant scale of multiple PCMs (cascaded) vs. single PCM configuration for thermal energy storage. Renewable Energy. 2015; 83:729-36.

[11]. Yuan F, Li MJ, Ma Z, Jin B, Liu Z. Experimental study on thermal performance of high-temperature molten salt cascaded latent heat thermal energy storage system. International Journal of Heat and Mass Transfer. 2018; 118:997-1011.

[12]. Khor JO, Sze JY, Li Y, Romagnoli A. Overcharging of a cascaded packed bed thermal energy storage: Effects and solutions. Renewable and Sustainable Energy Reviews. 2020; 117:109421.

[13]. Aldoss TK, Rahman MM. Comparison between the single-PCM and multi-PCM thermal energy storage design. Energy conversion and management. 2014;83:79-87.

[14]. Yang L, Zhang XS. Performance of a new packed bed using stratified phase change capsules. International Journal of Low-Carbon Technologies. 2012;7(3):208-14.

[15]. Mohammadnejad F, Hossainpour S. A CFD modeling and investigation of a packed bed of high temperature phase change materials (PCMs) with different layer configurations. Journal of Energy Storage. 2020;28:101209.

[16]. Li W, Wang J, Zhang X, Liu X, Dong H. Experimental and numerical investigation of the melting process and heat transfer characteristics of multiple phase change materials. International Journal of Energy Research. 2020;1–14.

[17]. Aguilar-Jiménez JA, Velázquez N, Acuña A, López-Zavala R, González-Uribe LA. Effect of orientation of a CPC with concentric tube on efficiency. Applied Thermal Engineering. 2018; 130:221-9.

[18]. Sobhansarbandi S, Atikol U. Performance of flat-plate and compound parabolic concentrating solar collectors in underfloor heating systems. Journal of Solar Energy Engineering. 2015; 137(3).

[19]. Zheng W, Yang L, Zhang H, You S, Zhu C. Numerical and experimental investigation on a new type of compound parabolic concentrator solar collector. Energy Conversion and Management. 2016; 129:11-22.

[20]. Ustaoglu A, Okajima J, Zhang XR, Maruyama S. Truncation effects in an evacuated compound parabolic and involute concentrator with experimental and analytical investigations. Applied Thermal Engineering. 2018; 138:433-45.

[21]. Li L, Wang B, Pottas J, Lipiński W. Design of a compound parabolic concentrator for a multi-source high-flux solar simulator. Solar Energy. 2019; 183:805-11.

[22]. Xia ET, Chen F. Analyzing thermal properties of solar evacuated tube arrays coupled with mini-compound parabolic concentrator. Renewable Energy. 2020; 153:155-67.